machines

MDPI

Article

Performance Optimization and Simulation Test of No-Tillage Corn Precision Planter Based on Discrete Element Method (DEM)

Jingyu Yang [1,†], Hailong Wu [1,†], Anfu Guo [1,*], Regis Rugerinyange [2], Chang Liu [1], Zhengyu Zhao [1], Wenchao Han [1] and Lvfa Yin [1]

[1] School of Mechanical and Automotive Engineering, Liaocheng University, Liaocheng 252000, China; 2021404977@stu.lcu.edu.cn (J.Y.); 2220230102@stu.lcu.edu.cn (H.W.); 2021400342@stu.lcu.edu.cn (C.L.); 2021404994@stu.lcu.edu.cn (Z.Z.); 2021405056@stu.lcu.edu.cn (W.H.); 2022400580@stu.lcu.edu.cn (L.Y.)
[2] Department of Mechanical and Manufacturing Engineering, Miami University, Oxford, OH 45056, USA; rugerir@miamioh.edu
* Correspondence: guoanfu@lcu.edu.cn
† These authors contributed equally to this work.

Abstract: In order to test the influence of the structural design of a no-tillage corn precision planter on vibration stability performance, a vibration model was constructed with the help of MATLAB/Simulink, and it was concluded that the vibration response curve of the no-tillage corn precision planter was relatively smooth. Based on the theory of the discrete element method (DEM), taking the planting apparatus of the no-tillage corn precision planter as the research object, firstly, a DEM single-factor test was carried out to investigate the effects of the slot inclination angle, number of slots, and rotational speed of the planter plate on the disturbance performance. Then, a three-factor, three-level orthogonal test was conducted with the maximum amount of seed discharging, the minimum average speed, and the minimum average kinetic energy as the final optimization objectives, and the qualified rate of seed discharging and the leakage rate as the evaluation indexes. The results show that the larger the inclination angle, the higher the number of slots, and the faster the rotational speed, the more violent the particle disturbance. At the same time, when the slot inclination angle of the planter plate is 60°, the number of slots is 20, and the rotational speed is 55 rpm, the seed discharge efficiency is the highest, at this time, the seed discharge qualification rate of maize particles is 95%, and the leakage rate is 3%; the results of this test can provide technical support for the research of the same kind of precision sowing equipment in the future.

Keywords: no-tillage corn precision planter; planter plate; discrete element method; simulation test; seed dispensing index

Citation: Yang, J.; Wu, H.; Guo, A.; Rugerinyange, R.; Liu, C.; Zhao, Z.; Han, W.; Yin, L. Performance Optimization and Simulation Test of No-Tillage Corn Precision Planter Based on Discrete Element Method (DEM). *Machines* **2024**, *12*, 465. https://doi.org/10.3390/machines12070465

Academic Editor: Zhuming Bi

Received: 13 May 2024
Revised: 24 June 2024
Accepted: 9 July 2024
Published: 10 July 2024

1. Introduction

Maize is the largest crop sown in China, and its production is crucial to ensure food security and economic stability in the world [1–3]. Sowing is the initial stage of agricultural production, as well as the most basic and critical stage, and it plays a decisive role in the green production of maize [4]. Mechanized planting technology helps to improve sowing efficiency and increase maize yield, and most of the mechanical systems have automatic control functions, which can reasonably set the depth of maize sowing and seed distribution, effectively reduce errors, reduce labor intensity, and improve work efficiency [5–7]. Although mechanical sowing is affected by many factors, precision seeding technology is always one of the most important processes in production. With seeding rate, plant spacing, and seeding depth as the core control objectives, precision sowing technology is the main mode of modern standardized maize production [8–10]. Therefore, in this paper, a no-tillage corn precision sowing machine was designed with the aim of

improving the soil organic matter content, constructing a fertile tillage layer, and increasing crop yields, among other things [11,12].

The discrete element method (DEM) is an analytical method based on molecular dynamics' principles for the study of force interactions and laws of motion between discrete materials. The DEM calculates particle–particle and particle–material contact forces based on the overlap terms between particles in a soft-sphere model and presents the motion of the entire particle system by sequentially updating the velocity and position of each particle [10,13].

At present, many researchers have carried out a great deal of research on various aspects of the structural performance and algorithmic control of the seeder, and they have achieved remarkable results [14]. For example, Li et al. [15] conducted virtual seeding simulation experiments on the designed single-row pneumatic combination seeder and set the working parameters so that the working performance of the combination seeder reaches the optimal level, which provides a reference for the development of precision seeding machines for small seeds and vegetables; Zou et al. [16] carried out a dynamic analysis of the main force components of the precision seeder for hole-tray seedlings, optimized the structure of the precision seeder and improved the motion performance of the planter, which is of great significance for achieving precision seeding in automated assembly lines; Chen et al. [17] tested different evaluation indexes of the designed precision maize planter based on CAN open protocol, verified the stability of the control system, and helped to improve the performance of the planter; Bacaicoa et al. [18] designed a rollover test bed to simulate different directions of static and dynamic rollover to determine the tilt angle of the vehicle that triggers the ATV-Quad rollover; Kim et al. [19] established a 3D simulation model of a self-propelled radish harvester, which is able to satisfy the standard angle under the additional load, and investigated the stability of the self-propelled radish harvester. However, there are fewer studies on discrete element analysis of no-tillage-type precision corn planters, as the rotational speed of the seed disc in the planter plate will affect the sowing quality of corn seeds, based on the seed grouting mechanism of the planter plate [20]; this paper mainly focuses on the structural analysis of the planter plate and the discrete element simulation.

We designed the key structure of the no-tillage corn precision planter, and for the stability problem of the structural design we used the MATLAB/Simulink (2020) function to build the relevant dynamic vibration model, established the vibration equations of the system, and analyzed the vibration characteristics of the no-tillage corn precision planter system. Based on the theory of the discrete element method (DEM), we carried out DEM single factor tests and three-factor, three-level orthogonal tests on the influence of the groove inclination angle, groove number, and rotation speed of the seeding plate on disturbance performance. When the slot inclination angle of the planter plate is larger, the number of slots is larger, and the rotational speed is faster, the disturbance of corn kernels is more intense. At the same time, the slot inclination angle of the planter plate is 60°, the number of slots is 15, and the rotational speed is 35 rpm, which is the optimal combination for the orthogonal test, and the planter plate efficiency of maize grain is the highest; at this time, the seed discharge qualification rate of maize particles is 95%, and the leakage rate is 3%. The qualification rate of the existing high-speed tilting corn seeder is 92.83% [20], while the qualification rate of the seeder of the no-tillage corn precision planter in this paper is 95%; the seeding efficiency of the no-tillage corn precision planter in this paper is greatly improved compared with that of the traditional seeder. The results of the discrete element simulation analysis of the no-tillage corn precision planter provide technical support for the parameter setting and research of similar precision corn seeding equipment in the future.

2. Simulation Modelling and Analysis Methods

2.1. Structure Analysis and Working Principle

2.1.1. Structure and Working Principle of No-Tillage Corn Precision Planter

The main structure of the no-tillage corn precision planter includes the following: rotary ploughing mechanism, feed forward program controller mechanism, seeding mechanism, mulching mechanism, and frame. The overall structure schematic diagram is shown in Figure 1a, and the technical parameters are shown in Table 1.

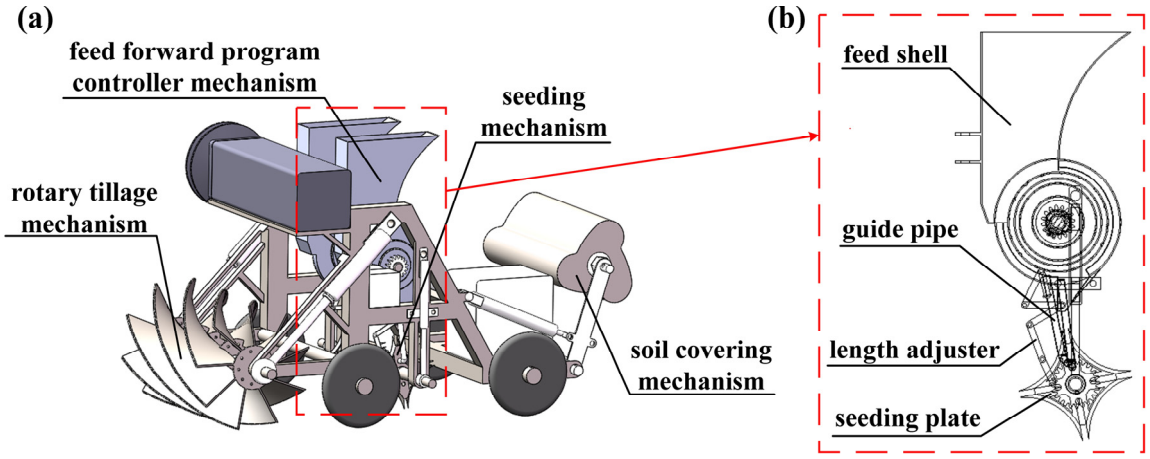

Figure 1. Structure of no-tillage corn precision planter. (**a**) 3D graphic of a no-tillage corn precision planter; (**b**) 2D graphic of a no-tillage corn precision planter seed discharge mechanism and seeding mechanism.

Table 1. Main parameters of no-tillage corn precision planter.

Norm	Overall Quality/(kg)	Overall Volume/(mm)	Line Spacing Range/(mm)
Digital	≤50	820 × 450 × 440	350–600

In the working process of the no-tillage corn precision planter, the electric motor drives the rotary ploughing mechanism and the seed discharge mechanism, and causes the seeding mechanism to rotate; the hydraulic pump provides oil pressure for them, which makes the hydraulic rod in the hydraulic cylinder push the rotary ploughing mechanism and the seeding mechanism, and causes the mulching mechanism to move. The rotary ploughing mechanism performs soil ploughing. Corn seeds enter the seeding mechanism through the seed discharge mechanism and the guide tube acts as a pipeline for the connection between the two; when the blade of the seeding disc in the seeding mechanism arrives at a certain spacing of the seed pit, the corn seeds in the seeding disc enter the seed pit, completing the seed discharge and seeding operations. The mulching mechanism fills the surrounding soil into the seed pit and tamps the soil. The feed forward program controller mechanism and the seeding mechanism are located in the middle position of the no-tillage corn precision planter; the two mechanisms are shown in Figure 1b.

2.1.2. Mechanism of Operation of the Planter Plate

In order to improve the seeding quality of the seed metering device in the no-tillage corn precision planter, we focus on the design of the parameters that affect the seeding results, such as the groove angle, groove number, and rotation speed of the planter plate. In order to study the influence of the structure of the planter plate on seed mobility and seed filling performance, the structure of three types of planter plates with different inclination angles was preliminarily designed for stress comparison simulation tests. The structure of the planter plate is shown schematically in Figure 2 [1].

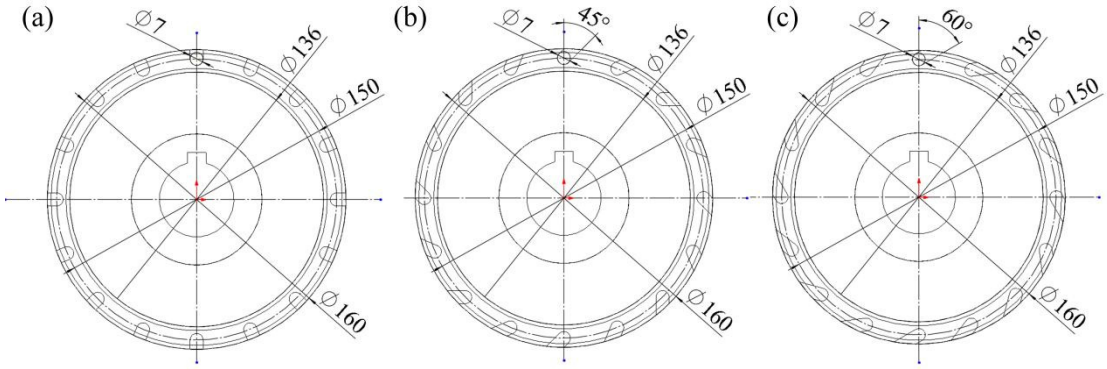

Figure 2. Structural sketches of three different inclination angles of planter plates. (**a**) 0° slot inclination; (**b**) 45° slot inclination; (**c**) 60° slot inclination.

2.2. Establishment and Analysis of Vibration Model

2.2.1. Establishment of Mathematical Model

Based on the vibration characteristics of the no-tillage corn precision planter in the vertical direction, a vibration response model of the no-tillage corn precision planter was constructed [21], and the whole of the no-tillage corn precision planter, except for the wheels, was regarded as the object under study. The wheels were regarded as a spring system and a damping system, and the vibration system was subjected to vertical upward excitation force, vertical downward elasticity and damping force, and vertical upward acceleration; its vibration response is shown in Figure 3.

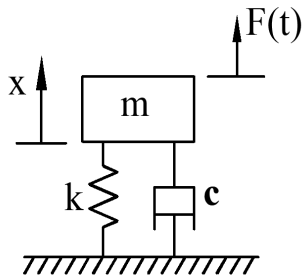

Figure 3. Vibration response model of no-tillage corn precision planter.

Dynamics Equation (1) is established based on the vibration response model of the no-tillage-type corn precision planter as:

$$F(t) - kx - c\dot{x} = m\ddot{x}, \tag{1}$$

transformed into the standard Equation (2) form, i.e.,

$$m\ddot{x} + c\dot{x} + kx = F(t), \tag{2}$$

where $F(t)$ denotes the forced vibration excitation force, k denotes the equivalent stiffness, c denotes the equivalent damping coefficient, m denotes the overall mass, x denotes the displacement, $\dot{x}$ denotes the velocity, and $\ddot{x}$ denotes the acceleration.

From the design parameters of the no-tillage corn precision planter in Table 1, we know that the mass of the no-tillage corn precision planter is approximately m = 50 kg, and the equivalent stiffness is taken as $k = 1 \times 10^4$ N/m. Since $0.03 \leq \xi \leq 0.07$, the equivalent damping coefficient, ξ = 0.05, is taken.

2.2.2. Simulink Module Construction

The main influencing factors of vibration and the fundamental wave of vibration signal are the prerequisites for the establishment of the vibration mathematical model. The

amplitude–frequency characteristics of vibration response is one of the most important methods for evaluating the dynamic response of the structure, which uses Fourier transform to transform the structural dynamic differential equations from the time domain to the frequency domain analysis, so that it can be evaluated intuitively at a certain excitation frequency of the dynamic response of the structure [22].

In this paper, based on the powerful simulation function of Simulink, the basic parameters of the Simulink module are set to establish the Simulink model of a single-degree-of-freedom no-tillage corn precision planter, as shown in Figure 4.

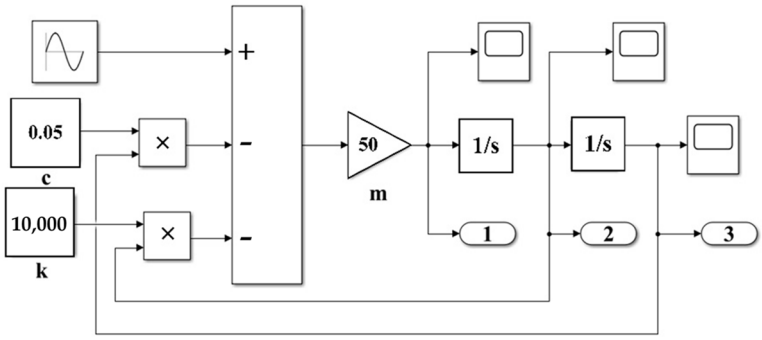

Figure 4. Simulink model of single-degree-of-freedom no-tillage corn precision planter.

2.3. Finite Element Analysis of Planter Plates

As shown in Figure 5, corn seeds are subjected to three forces: the extrusion stress of seed clusters (σ_1), the seed gravity stress (σ_2), and the centrifugal stress (σ_3) generated by the rotation of the planter plate in the inner cavity of the planter plate [23,24]. Corn seeds are gathered in the planting apparatus, and with the accelerated rotation of the planter plate the corn seeds move to the planter plate outlet under the action of the three stresses, the corn seeds will be thrown out at a certain speed along the tangential direction of the outlet, and the seeding process will be completed in turn.

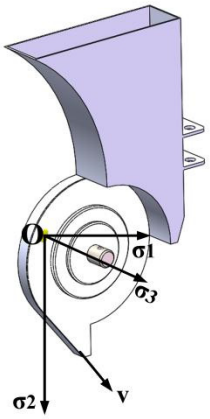

Figure 5. Seeding process of maize grain.

Since the vibration of the no-tillage corn precision planter is stable, the mechanical stress analysis of the planter plate is carried out without considering the vibration condition. In order to examine the stresses on the seed displacer disc under different slot inclination conditions, finite element analysis of the seed displacer disc is carried out using SolidWorks/Simulink. The material of the planter plate is alloy steel, and the yield strength is 6.204×10^8 N/m^2. The seed tray with 0° slot inclination was selected, fixed hinge constraints were added to the center hole part of the seed tray, centrifugal force with an angular velocity of 35 rad/s was applied, and 1 N force was applied inside the outer ring hole, and then rough-medium-fine meshing was performed. There were slight differences in the stress results generated by the three different numbers of discretization

nodes, as shown in Figure 6. As the number of discretization nodes increases, the results of stress analysis become more obvious. For the same part with different inclination angles, we adopt the same constraints and set the number of discretized nodes uniformly in the SolidWorks (2020) software, i.e., the mesh is automatically generated according to the size of the part; the stress cloud of the seed discharge disc is shown in Figure 7. The stress at the keyway of the seed discharge disc is the largest, and the stress is gradually decreasing outward in a ring shape; the stress at the peripheral grooves of the seed discharge disc is larger, and the yield force of the material is 6.204×10^8 N/m^2. The yield force of the material is 6.204×10^8 N/m^2. In the three different groove inclination states, the stress at the groove and keyway decreases with the increase of inclination; the stress value is lower than the yield force, which meets the stress design requirements.

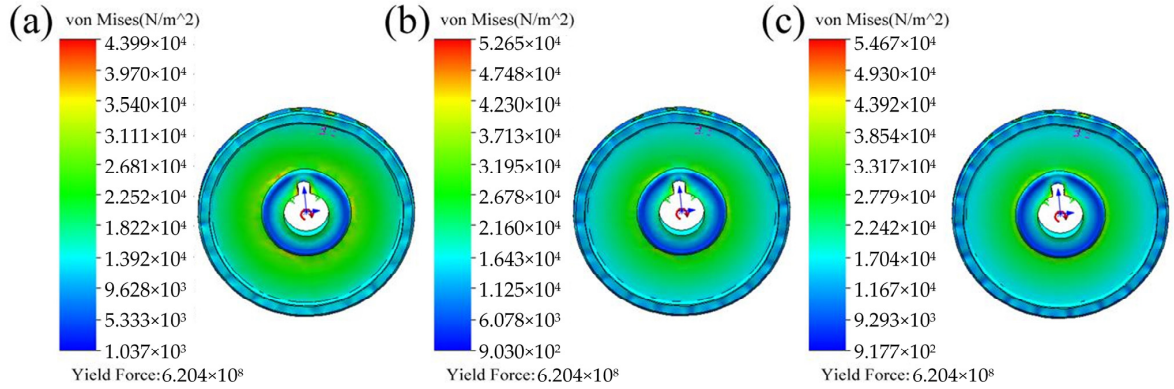

Figure 6. Mesh delineation of 0° inclined seed discharge discs. (**a**) Density rough mesh; (**b**) Density medium mesh; (**c**) Density good mesh.

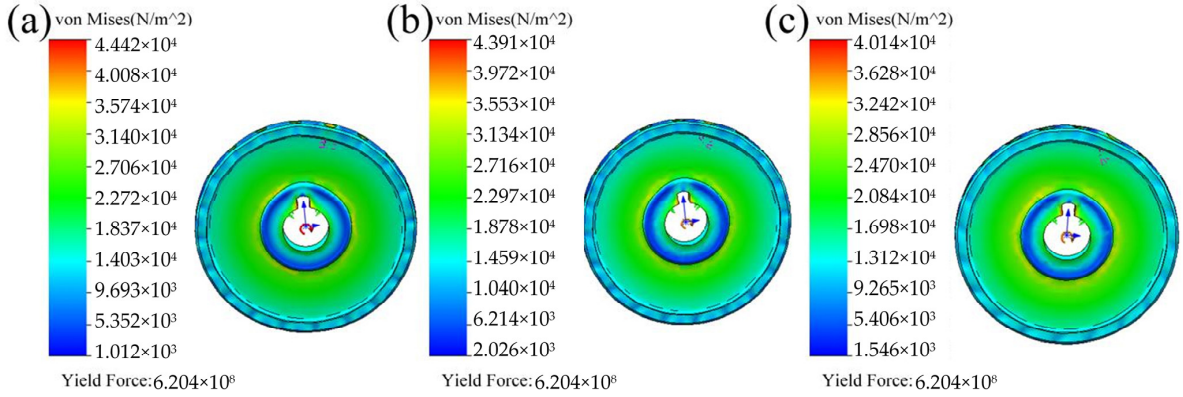

Figure 7. Stress analysis of planter plate. (**a**) 0° slot inclination; (**b**) 45° slot inclination; (**c**) 60° slot inclination.

2.4. Discrete Element Simulation Modelling and Parameter Setting

The discrete element method is a numerical simulation and computational method used to analyze the motion behavior and mechanical properties of particles and is widely used in the discretization of particulate matter and the optimization of grain detachment mechanisms [25–27], e.g., for the simulation of the threshing of crops such as wheat [28–30], rice [31,32], and cereals [33,34]. Since the process of seed discharging by the planter plate is similar to the process of grain detachment, this paper analyses the various motion indexes and disturbances of corn kernels in the planter plate by discrete element method.

The seed delivery and migration process of the no-tillage corn precision planter is divided into three stages: throwing out of the planting apparatus, moving in the guide tube, and throwing out of the seeding plate. The main components include the planting apparatus, the guide tube, and the seeding plate. The guide tube is closely connected

with the seeding plate, and the seeding–inoculation operation is carried out with the planting apparatus under the action of the length regulator. Simulation of the discrete movements of maize grains in the seed discharge tray was carried out using EDEM. Multi-spherical aggregates were chosen to characterize the movement of maize seeds and the filling processes [20], and the movement of maize particles in the planter plate was mainly investigated experimentally; the trajectory of maize particles is shown in Figure 8a. Multiple soft ball models with a diameter of 2 mm were connected and scaled to construct irregularly shaped corn seed particle models of different sizes, as shown in Figure 8b. Using the user-defined mode of particle distribution in EDEM, several soft sphere models with radius, R, of 1.5 mm were connected and scaled to construct irregularly shaped maize seed particle models of different sizes, as shown in Figure 8b. After the particle parameters are set up, the particle motion situation is carried out; the step size is set to 7.26×10^{-6} s and the total time is 2 s. After that, block structured meshing is carried out for the planter plate and the planter plate is divided into a large rectangle. According to the size of the particles, the software automatically gives the appropriate mesh size; in this paper, we use the mesh size of 2.5 R min. Finally, the particle simulation is carried out by the EDEM automatically to simulate the motion of the particles.

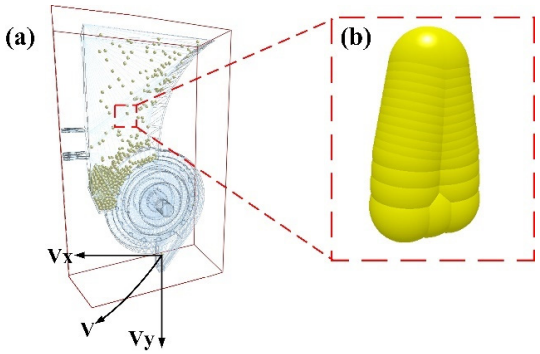

Figure 8. Motion of maize grains. (**a**) Simulation of the motion trajectory of corn grain; (**b**) Model of corn grain.

The simulation consisted of two materials, corn grain and seed dispenser, and the properties of the corn grain and seed dispenser components and the contact coefficients between the materials were set according to the literature [2]. The detailed parameter settings are shown in Table 2.

Table 2. Discrete element simulation parameters.

Sports Event	Corn Pellets		Steel
Poisson's Ratio	0.4		0.3
Shear Modulus/MPa	117		70,000
Density/(kg·m^{-3})	1180		7800
Contact Mechanical Parameters	Crash Recovery Factor	Corn Pellets-Steel	0.6
		Corn Pellets–Corn Pellets	0.182
	Coefficient of Static Friction	Corn Pellets–Steel	0.3
		Corn Pellets–Corn Pellets	0.431
	Coefficient of Kinetic Friction	Corn Pellets–Steel	0.01
		Corn Pellets–Corn Pellets	0.0782

According to Zhang Jianping et al. [35], after the corn seeds are detached from the planter plate, most of the seeds are discharged tangentially along the inner cavity distribu-

tion circle of the planter plate. The equations regarding the trajectory of the corn particles in the planter plate are shown in Equations (3)–(7).

$$V_0 = \omega R \tag{3}$$

$$x = V_0 + V_x \cdot t \tag{4}$$

$$y = V_y t + \frac{1}{2} g t^2 \tag{5}$$

$$V_x = \omega R sin\theta \tag{6}$$

$$V_y = \omega R cos\theta \tag{7}$$

where (x, y) is the coordinate position of the corn grain at a certain moment; ω is the rotational speed of the planter plate; R is the radius of the planter plate; V_x is the velocity component in the x-direction; V_y is the velocity component in the y-direction; g is the gravitational acceleration; t is the time; and θ is the angle between the velocity, V, and the vertical direction [36].

2.5. Methods of Orthogonal Testing

According to the requirements put forward in JB/T 10293-2001, Technical Conditions for the Single Grain (Precision) Seeder, the seeding qualification index is ≥80.0% and the leakage index is ≤15.0%. Taking the maximum seed qualification rate (Q) and the minimum leakage rate (L) as the final optimization objectives, the slot inclination angle, number of slots, and rotational speed of the planter plate are regarded as the A, B, and C factors, and a parametric mathematical model is established to seek the optimal solution under the boundary conditions of various factors. The equations of objective function and constraint condition are established as follows in Equation (8).

$$\begin{cases} \begin{cases} maxf(A,B,C) \\ ming(A,B,C) \end{cases} \\ s.t. \begin{cases} A = \{0, 45, 60\} \\ B = \{10, 15, 20\} \\ C = \{35, 45, 55\} \end{cases} \end{cases} \tag{8}$$

A 3 × 3 orthogonal test was conducted based on factor A, factor B, and factor C. The L9.3.4 orthogonal table was generated from the three levels of the three factors; the data of the nine experiments are shown in Table 3. The levels of 1, 2, and 3 for factor A (slot inclination angle of the planter plates) denote 0°, 45°, and 60°, respectively; the levels of 1, 2, and 3 for factor B (the number of slots of the planter plates) denote 10, 15, and 20, respectively; and the levels of 1, 2, and 3 for factor C (rotational speed of planter plate) at levels 1, 2, and 3 indicate 35, 45, and 55 rpm, respectively.

Table 3. Experimental Data.

Test Mark	Factor A (Inclination)	Factor B (Number of Grooves)	Factor C (Rotation Speed)	Number of Particles	Velocity	Kinetic Energy
1	1	1	1	0.10	0.60	6.09×10^{-5}
2	1	2	3	0.10	0.66	5.06×10^{-5}
3	1	3	2	0.15	0.98	1.26×10^{-4}
4	2	1	3	0.15	0.81	6.86×10^{-5}
5	2	2	2	0.15	0.62	4.91×10^{-5}
6	2	3	1	0.10	0.62	5.23×10^{-5}
7	3	1	2	0.30	0.58	4.41×10^{-5}
8	3	2	1	0.55	0.88	7.65×10^{-5}
9	3	3	3	0.60	0.61	5.15×10^{-5}

3. Results and Discussion

3.1. Analysis of Results for Vibration Stability

The autocorrelation function of the vibration signals collected during the operation of the no-tillage corn precision planter has the characteristics of positive and cosine function distribution [37,38]; the simulation results are shown in Figure 9. The vibration displacements of the no-tillage corn precision planter under the action of the forced vibration are all positive, which indicates that the vibration occurs before the equilibrium position; with the increase of time, the vibration system is gradually far away from the equilibrium position, and the change of the displacements decreases continuously. Vibration velocity and vibration acceleration have positive values. The values of vibration velocity and vibration acceleration are both positive and negative, the acceleration at the equilibrium position is the largest, and the vibration velocity curve changes less compared with the vibration acceleration curve. Taken together, the vibration displacement, vibration velocity, and vibration acceleration curves have very small variations. As a result, the motion trajectory curve of the single-degree-of-freedom forced vibration system using MATLAB/Simulink meets the vibration stability requirements of the no-tillage corn precision planter, which verifies the correctness of the simulation results of the model and the objectivity of the vibration law of the single-degree-of-freedom forced vibration system [4].

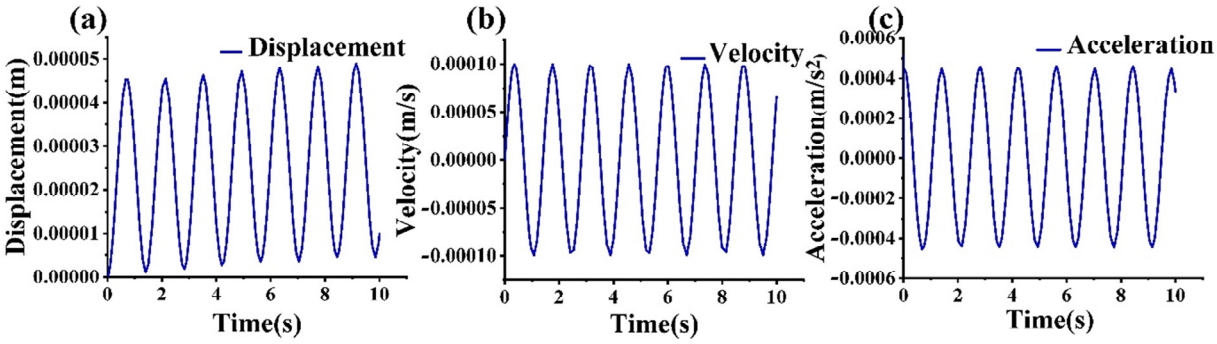

Figure 9. Simulation results. (**a**) Vibration displacement response curve; (**b**) Vibration velocity response curve; (**c**) Vibration acceleration response curve.

3.2. Effect of One-Factor Test on Perturbation Performance

Pearson Correlation is a measure of vector similarity. The output ranges from −1 to +1, with 0 representing no correlation, negative values being negative correlation, and positive values being positive correlation. In order to study the influencing factors of the severe disturbance of corn particles in the planting apparatus, we took the groove inclination angle, groove number, and rotation speed of the planter plate as the research object and used the number of corn particles in the planting apparatus, the average speed, and the average kinetic energy as the evaluation indexes, and carried out the correlation analysis between the parameters of the seed metering plate and the disturbance of corn particles.

3.2.1. Effect of Slot Inclination on Disturbance Performance

The number of slots in the planter plate was set to 20 and the rotational speed was set to 75 rpm. The Pearson Correlation indicated the strength of the correlation between the slot inclination of the planter plate and the number of corn particles discharged, and the average velocity and the average kinetic energy, as shown in Table 4. The correlation coefficients between inclination and number of particles, velocity, and kinetic energy were all significant. Kinetic energy values were all significant, with correlation coefficient values of 0.763, 0.742, and 0.657, respectively, and the correlation coefficient values were all greater than 0, which implies that there is a positive correlation between inclination and number of particles, velocity, and kinetic energy, i.e., the number of planter plates has a positive correlation with the number of particles. The correlation coefficients were all greater than 0, meaning that there was a positive relationship between inclination and the number of

particles, velocity, and kinetic energy, i.e., the greater the inclination of the groove of the disc, the greater the number of particles, the greater the average velocity, and the greater the average kinetic energy.

Table 4. Pearson's Correlation at Different Inclinations—Standard Format.

	Average Value	Standard Deviation	Inclination	Number of Particles	Velocity	Kinetic Energy
Inclination	28.636	20.987	1			
Number of Particles	0.310	0.157	0.763 *	1		
Velocity	0.580	0.020	0.742 *	0.847 **	1	
Kinetic Energy	0.000	0.000	0.657 *	0.628 *	0.692 *	1

* $p < 0.05$ ** $p < 0.01$.

According to the literature [39], the inclination angle affects the seed disturbance performance. With other conditions such as the number of slots and rotational speed of the planter plate remaining unchanged, the effect of the inclination angle of the slots of the planter plate on each evaluation index is analyzed, and once the seed morphology in the grouting area is stable, simulated renderings of various inclinations are intercepted [40], as shown in Figure 10, where the different colors represent the different velocities of the seeds. At the same grouting volume, different slot inclinations of the planter plates result in different seed velocities and different seed mobility [41]. The velocity of movement of corn grains in Figure 10 shows that the change in velocity at the slot of the seed discharge disc with 0° inclination is significantly greater than the other two inclinations, and that the movement of corn grains is more violent, with greater disarray of corn grains in the seed discharger.

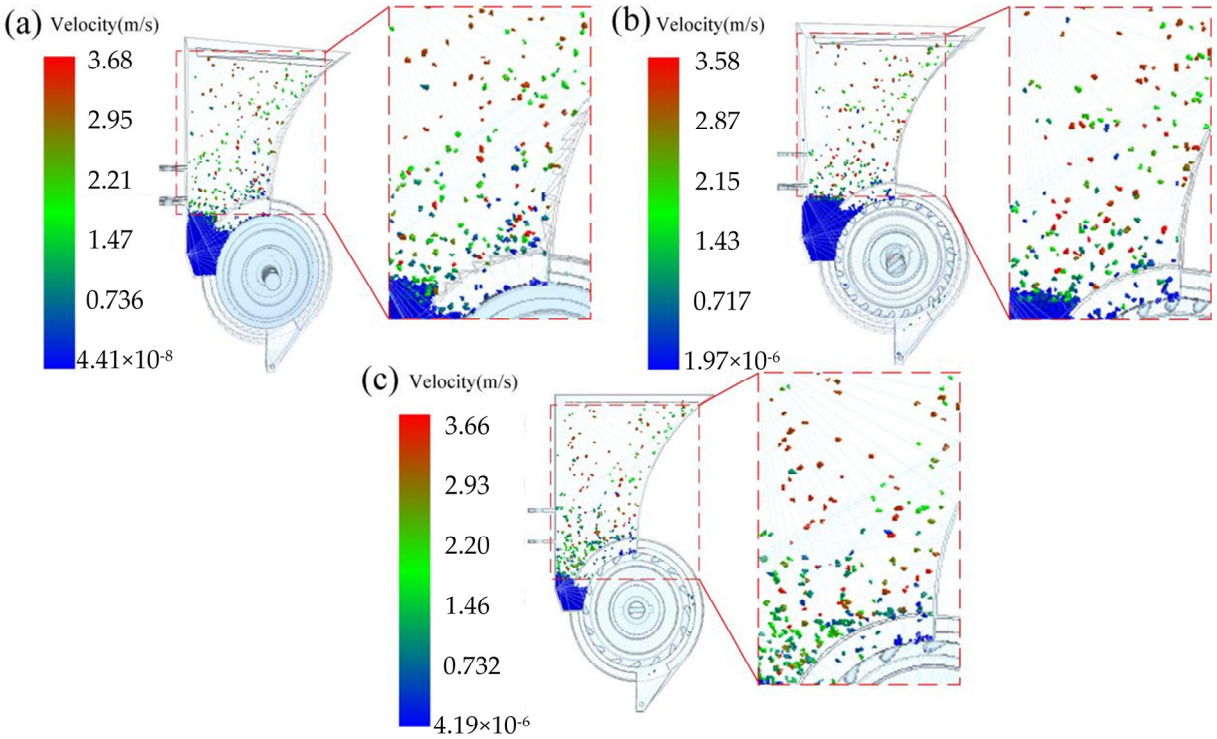

Figure 10. Disturbance effect diagrams for different inclination angles. (**a**) 0° inclination angle; (**b**) 45° inclination angle; (**c**) 60° inclination angle.

In order to more accurately describe the disturbance performance of the slot inclination of the seeder disc on corn seeds, we extracted EDEM simulation data for analysis [40]. The histograms of the number of corn seed particles discharged in the seeder with three different inclinations are shown in Figure 11, and the line graphs of the average velocity and average kinetic energy of the corn particles over time are shown in Figure 12. With the increase of the slot inclination angle, the number of corn particles discharged gradually increased, the average speed gradually increased, the average kinetic energy gradually increased, and the seed perturbation became more and more violent, consistent with the results of Pearson Correlation analysis. When the slot inclination angle is 45°, the number of seeds discharged is higher and it is not easy to see the situation of multiple grains in one hole, and the change of the average kinetic energy is relatively smooth.

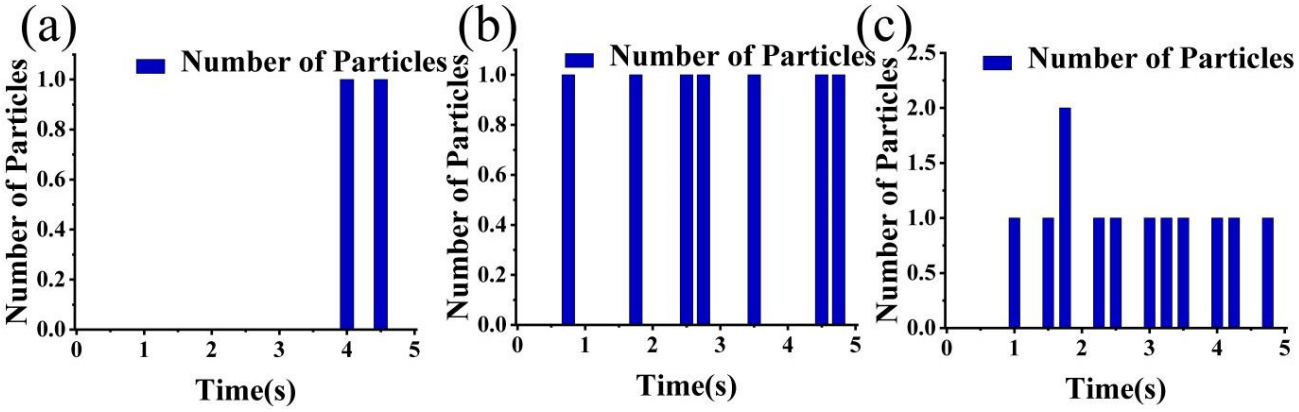

Figure 11. Histogram of the number of rows of seeds at different inclination angles. (**a**) 0° inclination angle; (**b**) 45° inclination angle; (**c**) 60° inclination angle.

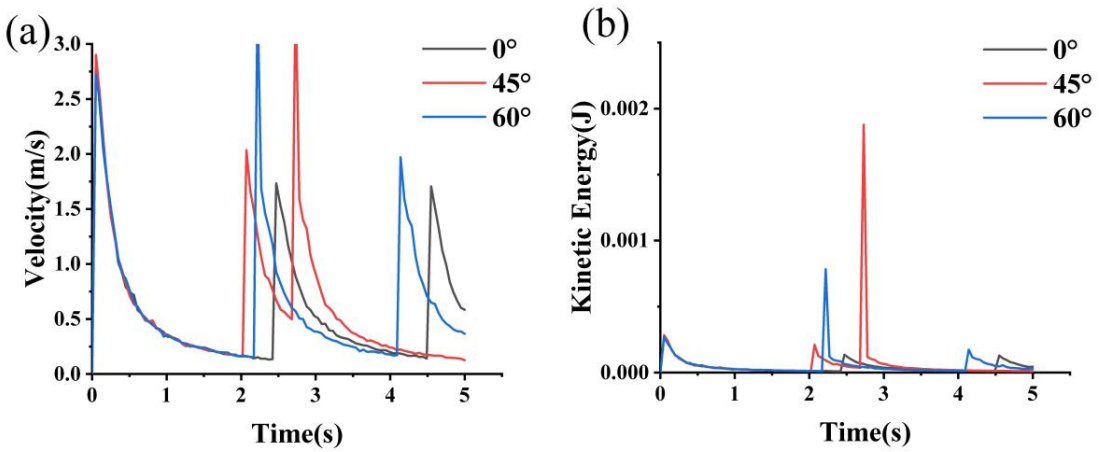

Figure 12. Line graphs of mean velocity and mean kinetic energy for different inclination states. (**a**) Mean velocity; (**b**) Mean kinetic energy.

3.2.2. Effect of Number of Slots on Perturbation Performance

The slot inclination of the planter plate was set at 60°, and the rotational speed of the planter plate was set at 75 rpm. Under other conditions, the strength of the correlation between the number of grooves of the planter plate and the number of seed particles discharged, the average velocity, and the average kinetic energy was investigated by using Pearson Correlation, as shown in Table 5. The correlation coefficient values (p) were 0.930, 0.713, and 0.719, respectively. Number of particles, velocity, and kinetic energy all show significance and the correlation coefficient values (p) of 0.930, 0.713, and 0.719, respectively, and the correlation coefficient values are all greater than 0, which means that the correlation between the number of grooves and the number of particles, velocity, and kinetic energy

show significance. Velocity and kinetic energy have a positive correlation between number of grooves and number of particles, velocity, and kinetic energy, i.e., the higher the number of grooves in the disc, the higher the number of seeds, the higher the average velocity, and the higher the average kinetic energy.

Table 5. Pearson's Correlation at Different Number of Slots—Standard Format.

	Average Value	Standard Deviation	Number of Grooves	Number of Particles	Velocity	Kinetic Energy
Number of Grooves	18.636	5.056	1			
Number of particles	0.527	0.188	0.930 **	1		
Velocity	0.609	0.078	0.713 *	0.694 *	1	
Kinetic Energy	0.003	0.009	0.719 *	0.674 *	0.867 **	1

* $p < 0.05$ ** $p < 0.01$.

In order to describe more accurately the disturbance performance of the number of slots of the seeding discs on the maize seeds in the planter plate, EDEM simulation data were extracted and analyzed. The perturbation of corn seeds in the seeder was analyzed for the number of slots of the seeding discs of 10, 15, and 20, while other conditions remained constant. The histograms of the number of slots of the seeding discs with different number of slots for the seeding particles in the planting apparatus are shown in Figure 13, and the line graphs of the average velocity and the average kinetic energy of the corn particles with respect to the time are shown in Figure 14.

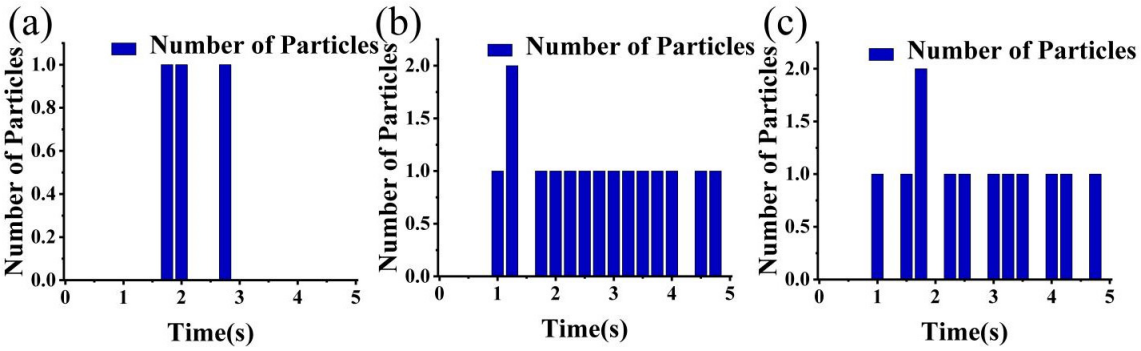

Figure 13. Histogram of the number of seeds discharged in different slot number states. (**a**) 10 slots; (**b**) 15 slots; (**c**) 20 slots.

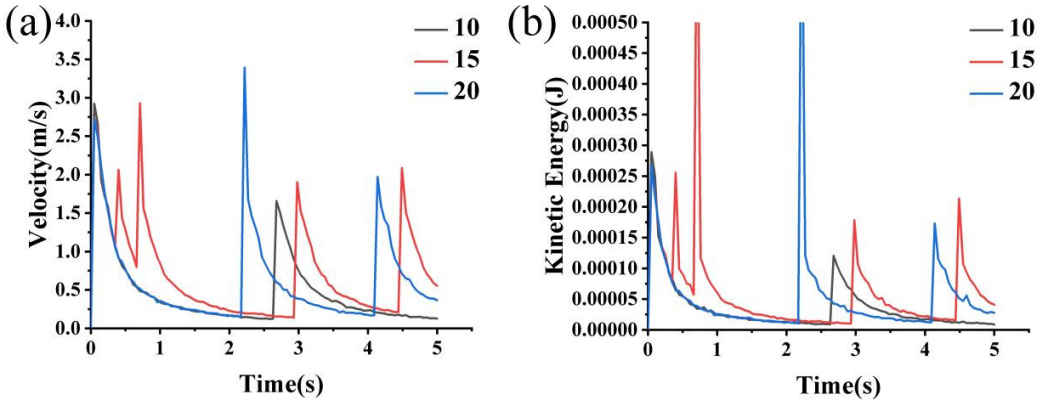

Figure 14. Line plots of mean velocity and mean kinetic energy for different notch states. (**a**) Mean velocity; (**b**) Mean kinetic energy.

With the increase of the number of slots in the planter plate, the number of seeds discharged gradually increased, the seed disturbance became more and more violent, and the average speed and average kinetic energy of corn kernels changed in the same trend with less ups and downs. If the number of slots is 10, the grain is more stable, but the number of seeds discharged is smaller. If the number of slots is 15, the seeds are discharged more evenly.

3.2.3. Influence of the Rotational Speed of the Planter Plate on Disturbance Performance

The slot inclination angle of the planter plate was set at 60°, the number of slots of the planter plate was set at 15, and under the other conditions remaining unchanged, Pearson Correlation was used to study the strength of the correlation between the rotational speed of the planter plate and the number of seed particles of maize in the planter plate, the average speed, and the average kinetic energy, as shown in Table 6. The three terms of rotation speed and number of particles, velocity, and kinetic energy showed significance, with correlation coefficient values (p) of 0.943, 0.953, and 0.956 respectively, and the correlation coefficient values were greater than 0, which means that there is a positive correlation between number of grooves and number of particles, velocity, and kinetic energy, i.e., the faster the rotational speed of the seed disc, the more seeds are discharged, the greater the average velocity, and the greater the average kinetic energy.

Table 6. Pearson's correlation at different rotational speeds—Standard Format.

	Average Value	Standard Deviation	Rotation Speed	Number of Particles	Velocity	Kinetic Energy
Rotation Speed	47.273	14.485	1			
Number of particles	0.525	0.142	0.943 **	1		
Velocity	0.541	0.171	0.953 **	0.976 **	1	
Kinetic Energy	0.000	0.000	0.956 **	0.979 **	0.972 **	1

** $p < 0.01$.

According to [42], the rotational speed of the planter plate affects the seed pass rate, and in order to describe more accurately the disturbance performance of the planter plate's rotational speed on the seeds, EDEM simulation data were extracted and analyzed. In the case of other conditions being unchanged, when the rotation speed of the planter plate is 35, 45, and 55 rpm, we analyze the disturbance of corn seeds in the planting apparatus. The histogram of the number of seeds discharged is shown in Figure 15, and the average speed and average kinetic energy of the corn seeds are shown in Figure 16.

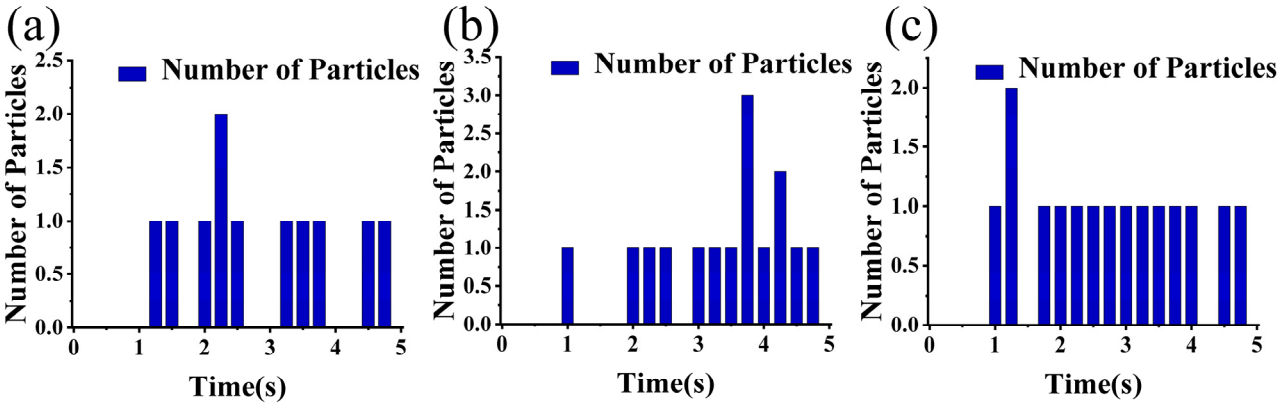

Figure 15. Histogram of the number of seeds discharged at different rotational speed states. (**a**) 35 rpm; (**b**) 45 rpm; (**c**) 55 rpm.

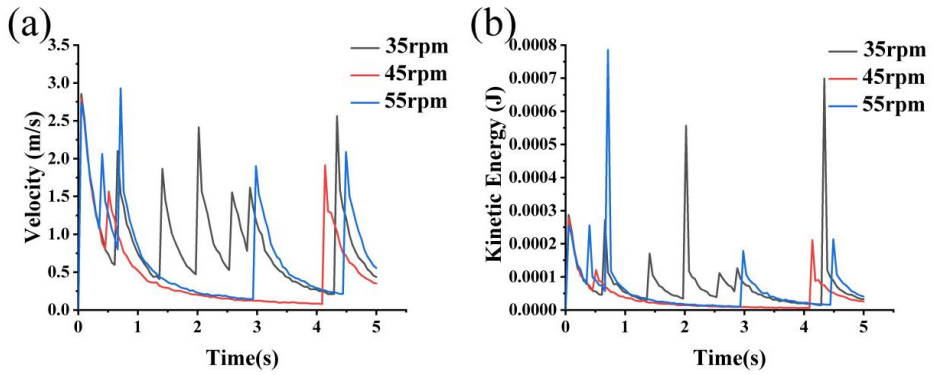

Figure 16. Line plots of mean velocity and mean kinetic energy for different speed states. (**a**) Mean velocity; (**b**) Mean kinetic energy.

As the speed of the seed discharging disc increases, the number of corn grains discharged gradually increases and the disturbances become more and more violent. At the same time, the time for the first corn grain to be discharged was gradually advanced, making it easier for seed leakage behavior to occur. The trend of the average velocity of corn particles in the planter plate was roughly the same, accelerating first and then decelerating. As the rotational speed increased, the rate of particle regeneration accelerated, the acceleration of the regenerated particles increased significantly, and the average kinetic energy of the particles changed less. As the corn particles landed, the frictional collision between the particles resulted in energy loss. The data show that the maximum energy difference of corn particles is 10^{-4} level, which is extremely small energy loss for no-tillage-type corn precision planters and meets the requirement of the era of energy saving and emission reduction.

3.3. Orthogonal Test Analysis

The experimental data after orthogonalization were subjected to polar analysis three times to find out the best combination of each level of the three factors. The K-value indicates the sum of the experimental data under the requested factor and level; K avg values indicate the corresponding mean values; the optimal level indicates the level number corresponding to the optimal K avg value of the requested factor; R denotes the extreme value of the factor, comparing the strengths and weaknesses of the factors, which equals the maximum value of K avg minus the minimum value of K avg at the time of the requested factor; the number of levels indicates the number of levels of the re-quested factor; and the number of replicates per level, r, indicates the average number of test replicates for the level. Firstly, the level of influence of the three factors on the number of rows of seeds was analyzed, and the specific data are shown in Table 7. When the combination of the three factors is 3, 3, 3, i.e., the slot inclination is 60°, the number of slots is 20, and the rotational speed is 55 rpm, the number of seed rows is the highest; the dominance of the specific levels among the factors is shown in Figure 17.

Table 7. Number of particles—extreme analysis.

Item	Level	Inclination	Number of Grooves	Rotation Speed
K-Value	1	0.35	0.55	0.75
	2	0.40	0.80	0.60
	3	1.45	0.85	0.85
K avg-Value	1	0.12	0.18	0.25
	2	0.13	0.27	0.20
	3	0.48	0.28	0.28
Optimum Level		3	3	3
R		0.25	0.37	0.10
Number of Levels		3	3	3
r (Number of Replicates Per Level)		3.0	3.0	3.0

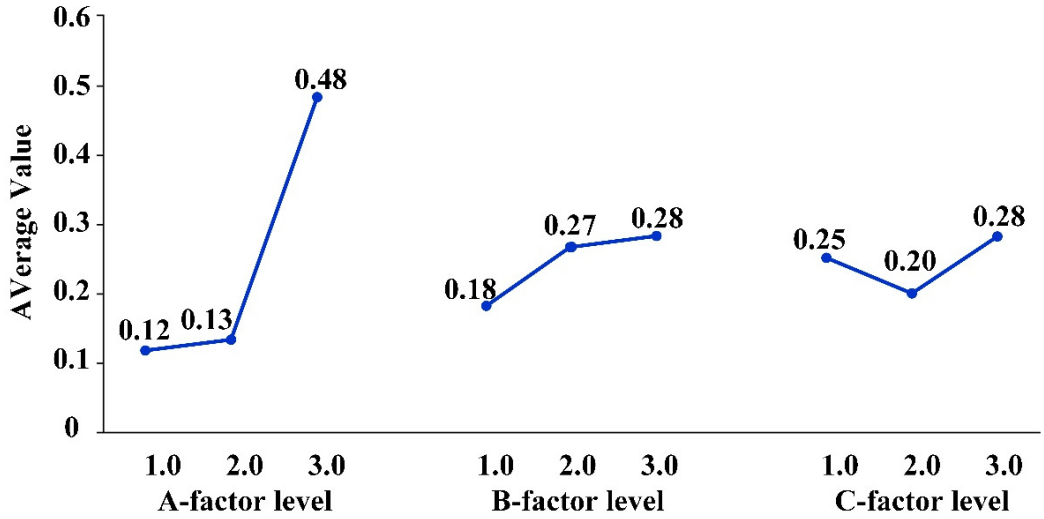

Figure 17. Plot of means of the number of rows at each level of the three factors.

Secondly, the degree of influence of the three factors on the average velocity of corn particles in the planter plate was analyzed, and the specific data are shown in Table 8. When the combination of the three factors is 1, 3, 2, i.e., when the slot inclination of the planter plate is 0°, the number of slots is 20, and the rotational speed is 45 rpm, the average velocity of maize particles in the planter plate is the greatest, and the particle disturbance is the most violent, the advantage of the specific level between the factors is shown in Figure 18.

Table 8. Velocity—extreme analysis.

Item	Level	Inclination	Number of Grooves	Rotation Speed
K-Value	1	2.24	1.99	2.10
	2	2.05	2.16	2.18
	3	2.07	2.21	2.08
K avg-Value	1	0.75	0.66	0.70
	2	0.68	0.72	0.73
	3	0.69	0.74	0.69
Optimum Level		1	3	2
R		0.06	0.07	0.03
Number of Levels		3	3	3
r (Number of Replicates Per Level)		3.0	3.0	3.0

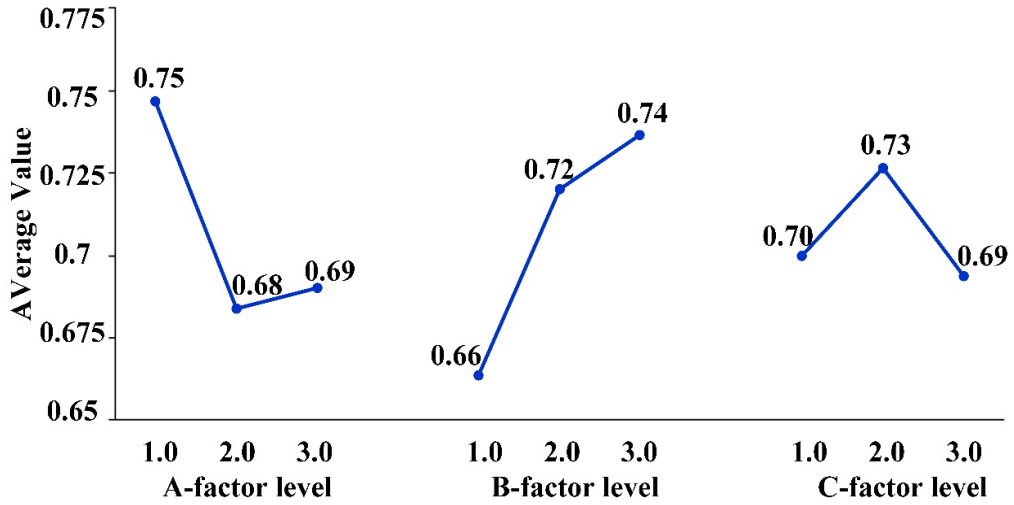

Figure 18. Plot of means of average speeds for each level of the three factors.

Finally, the degree of influence of the three factors on the average kinetic energy of corn kernels was analyzed, as shown in Table 9. When the combination of the three factors was 1, 3, 2, i.e., when the slot inclination of the planter plate was 0°, the number of slots was 20, and the rotational speed was 45 rpm, the average kinetic energy of maize particles in the planter plate was the greatest, and the particles were the most violently perturbed; the dominance of the specific levels among the factors is shown in Figure 19.

Table 9. Kinetic energy—extreme analysis.

Item	Level	Inclination	Number of Grooves	Rotation Speed
K-Value	1	2.37×10^{-4}	1.74×10^{-4}	1.90×10^{-4}
	2	1.70×10^{-4}	1.76×10^{-4}	2.18×10^{-4}
	3	1.72×10^{-4}	2.29×10^{-4}	1.71×10^{-4}
K avg-Value	1	7.92×10^{-5}	5.79×10^{-5}	6.32×10^{-5}
	2	5.67×10^{-5}	5.87×10^{-5}	7.30×10^{-5}
	3	5.74×10^{-5}	7.66×10^{-5}	5.69×10^{-5}
Optimum Level		1	3	2
R		2.25×10^{-5}	1.87×10^{-5}	1.61×10^{-5}
Number of Levels		3	3	3
r (Number of Replicates Per Level)		3.0	3.0	3.0

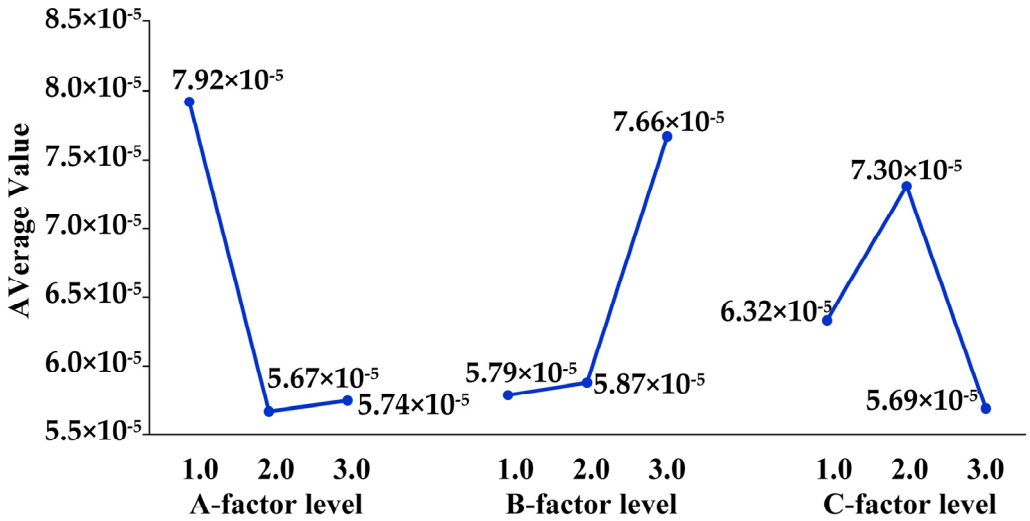

Figure 19. Plot of mean values of average kinetic energy for each level of the three factors.

Orthogonal test were performed on the slot inclination angle, number of slots, and rotational speed of the seed discharge disc, with the maximum number of seeds discharged, the minimum average speed, and the minimum average kinetic energy as the optimal orthogonal objective, combined with the mean value of each level of the three factors, when the slot inclination angle of the seed discharge disc is 60°, the number of slots is 20, and the rotational speed of 55 rpm is the optimal, with the largest number of seeds discharged, the average speed and the average kinetic energy is small, and the highest efficiency of seed discharging.

3.4. Experimental Verification of Sowing Accuracy

When the slot inclination of the planter plate is 60°, the number of slots is 20, and the rotational speed is 55 rpm, the changes in the number of corn kernels discharged in the planter plate, the average speed of corn kernels, and the average kinetic energy of corn kernels are shown in Figure 20. According to GB/T 6979-2005, Test Methods for Single Grain (Precision) Seeder, the seeding test of a no-tillage-type corn precision seeder was carried out, and each group of tests was repeated three times with 100 seeds each time.

The results were analyzed by taking the average value, and the test was carried out with the qualified index and the leakage index as the evaluation indexes of the seed discharge performance [43].

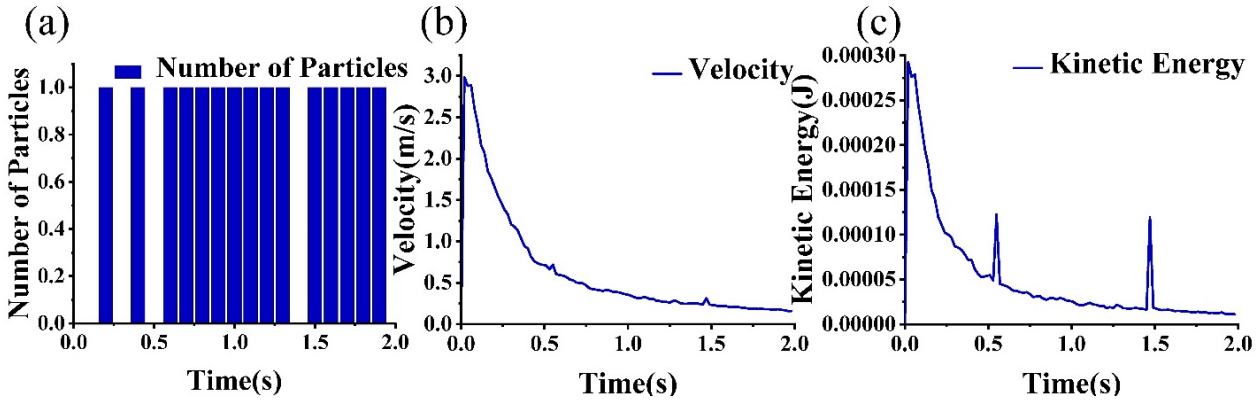

Figure 20. Three-factor variation of maize grain. (**a**) Plot of number of seeds in rows; (**b**) Plot of average velocity; (**c**) Plot of average kinetic energy.

When the slot inclination of the planter plate was 60°, the number of slots was 20 and the rotational speed was 55 rpm, the disturbance of the maize seeds in the planting apparatus was relatively smooth, the qualified rate of seed discharge was the highest, and the leakage rate was the lowest.; at this time, the qualified rate of maize kernel discharge was 95% and the leakage rate was 3%. The leakage rate increased with the increase of the rotational speed of the planter plate; under higher centrifugal inertial stress, the seed undergoes turbulence in the chamber and subsequently the parts of the seed squeeze each other and gather together, resulting in an increase in the leakage rate. The residence time of the seed in the outer ring of the planter plate decreases, resulting in most of the seed falling into the chamber, and the leakage rate gradually increases [20].

4. Conclusions

(1) In this paper, for the requirements of single-grain precision sowing, a no-tillage-type corn precision planter is designed to meet the modern sowing requirements, which can effectively solve the problems of obstructed sowing, inconsistent seed spacing, and low efficiency.

(2) According to the relevant principles of dynamics, the MATLAB/Simulink analysis of the no-tillage corn precision planter was carried out, and the device was designed to meet the structural requirements of stability.

(3) Using SolidWorks (2020) and EDEM (2022) software, we carry out finite element analysis of the planter plate and discrete element analysis of the corn seeds in the planter plate, and the results show the following: the resultant design of the planter plate is within the range of the yield force requirement, and the larger the slot inclination of the disc and the more slots, the larger the number of seeds discharged; the higher the rotational speed, the lower the number of seeds discharged; the larger the values of the slot inclination, the number of slots, and the rotational speed, the larger the values of slot inclination, number of slots and rotational speed, the larger the average speed and average kinetic energy.

(4) The discrete element method and Pearson Correlation analysis were used to simulate the seed discharging process of maize grains in the planter plate, and to study the strength of the correlation between the slot inclination, number of slots, and rotational speed of the discharging discs, and the number of seeds discharged, the average speed and the average kinetic energy.

(5) According to the optimal solution obtained from the three-factor, three-level orthogonal test, when the slot inclination of the planter plate is 60°, the number of slots is 20,

and the rotational speed is 55 rpm, the disturbance of maize seeds in the planting apparatus is relatively gentle, the qualified rate of seed discharging is the highest, and the leakage rate is the lowest; the qualified rate of seed discharging of maize grains is 95% and the leakage rate is 3%. The results of this experiment provide technical support for future parameter setting and research on similar precision maize seeding equipment.

Author Contributions: Conceptualization, J.Y. and Z.Z.; methodology, J.Y.; software, J.Y.; validation, J.Y., H.W. and C.L.; formal analysis, J.Y.; investigation, W.H.; resources, L.Y.; data curation, R.R.; writing—original draft preparation, J.Y.; writing—review and editing, H.W.; visualization, J.Y.; supervision, H.W.; project administration, J.Y.; funding acquisition, A.G. All authors have read and agreed to the published version of the manuscript.

Funding: This work is supported by Innovative Research Group Project of the National Natural Science Foundation of China (52075280), the Natural Science Foundation of Shandong Province (ZR2023ME154), and the Training Program of Innovation and Entrepreneurship for Undergraduates (Grant No. CXCY2023129, CXCY2023122).

Data Availability Statement: Data is contained within the article.

Acknowledgments: The authors thank the Innovative Research Group Project of the National Natural Science Foundation of China and the Natural Science Foundation of Shandong Province for providing financial support for this study.

Conflicts of Interest: The authors declare no conflicts of interest.

References

1. Reiner, W.; Nguyen, V.; Bui, T.; Martin, G.; Katherine, M.; Shabbir, H.; Bjoern, O. Carbon Footprint Calculator Customized for Rice Products: Concept and Characterization of Rice Value Chains in Southeast Asia. *Sustainability* **2022**, *14*, 315.
2. Ittisak, J.; Tawadchai, S.; Vikas, K. Assessing the Economic and Environmental Impact of Jasmine Rice Production: Life Cycle Assessment and Life Cycle Costs Analysis—ScienceDirect. *J. Clean. Prod.* **2021**, *303*, 127079.
3. Hu, Q.; Jiang, W.; Qiu, S.; Xing, Z.; Hu, Y.; Guo, B.; Liu, G.; Gao, H.; Zhang, H.; Wei, H. Effect of Wide-Narrow Row Arrangement in Mechanical Pot-Seedling Transplanting and Plant Density on Yield Formation and Grain Quality of Japonica Rice—ScienceDirect. *J. Integr. Agric.* **2020**, *19*, 1197–1214. [CrossRef]
4. Deng, F.; Zhang, C.; He, L.; Liao, S.; Li, Q.; Li, B.; Zhu, S.; Gao, Y.; Tao, Y.; Zhou, W.; et al. Delayed Sowing Date Improves the Quality of Mechanically Transplanted Rice by Optimizing Temperature Conditions during Growth Season—ScienceDirect. *Field Crops Res.* **2022**, *281*, 108493. [CrossRef]
5. Wang, Y. Research on the Hydraulic Control Design of Traction System of the Fertilizer Planter. *J. Agric. Mech. Res.* **2023**, *45*, 76–80.
6. Liu, K. Optimization analysis of fully automatic control system for corn planter. *New Agric.* **2022**, 13–14.
7. Wang, S.; Zhao, B.; Yi, S.; Zhao, X.; Liu, Z.; Sun, Y. Electric-driven mung bean precision seeder control system based on IGWO-LADRC. *Trans. Chin. Soc. Agric. Mach.* **2022**, *53*, 87–98.
8. Gao, X.; Cui, T.; Zhou, Z.; Yu, Y.; Xu, Y.; Zhang, D.; Song, W. DEM Study of Particle Motion in Novel High-Speed Seed Metering Device. *Adv. Powder Technol.* **2021**, *32*, 1438–1449. [CrossRef]
9. Jia, H.; Chen, Y.; Zhao, J.; Guo, M.; Huang, D.; Zhuang, J. Design and Key Parameter Optimization of an Agitated Soybean Seed Metering Device with Horizontal Seed Filling. *Int. J. Agric. Biol. Eng.* **2018**, *11*, 76–87. [CrossRef]
10. Xu, J.; Sun, S.; He, Z.; Wang, X.; Zeng, Z.; Li, J.; Wu, W. Design and Optimisation of Seed-Metering Plate of Air-Suction Vegetable Seed-Metering Device Based on DEM-CFD. *Biosyst. Eng.* **2023**, *230*, 277–300. [CrossRef]
11. Mengjie, G.; Jianye, L.; Jianyu, L.; Jiarui, Q.; Xingyi, Z. Changes of soil structure and function after 16-year conservation tillage in black soil. *Trans. Chin. Soc. Agric. Eng.* **2021**, *37*, 108–118.
12. Keshavarz Afshar, R.; Cabot, P.; Ippolito, J.A.; Dekamin, M.; Reed, B.; Doyle, H.; Fry, J. Corn Productivity and Soil Characteristic Alterations Following Transition from Conventional to Conservation Tillage. *Soil Tillage Res.* **2022**, *220*, 105351. [CrossRef]
13. Di Renzo, A.; Di Maio, F.P. Comparison of Contact-Force Models for the Simulation of Collisions in DEM-Based Granular Flow Codes. *Chem. Eng. Sci.* **2004**, *59*, 525–541. [CrossRef]
14. Ananda Rao, M.; Srinivas, J.; Rama Raju, V.B.V.; Kumar, K.V.S.S. Coupled Torsional–Lateral Vibration Analysis of Geared Shaft Systems Using Mode Synthesis. *J. Sound Vib.* **2003**, *261*, 359–364. [CrossRef]
15. Li, Y.; Bai, Y.; Zhang, X.; Xie, F. Structural Design and Simulation Analysis of a Dual-Row Pneumatic Vegetable Precision Planter. *Processes* **2023**, *11*, 1803. [CrossRef]
16. Zou, H.; Shen, Y.; Chen, Z.; Zhang, C.; Wang, M.; Wu, M. Structural Design and Kinetic Analysis of Precise Seed Planter for Tray Seedling. *E3S Web Conf.* **2023**, *438*, 01022. [CrossRef]

17. Chen, J.; Zhang, H.; Pan, F.; Du, M.; Ji, C. Control System of a Motor-Driven Precision no-tillage Maize Planter Based on the CANopen Protocol. *Agriculture* **2022**, *12*, 932. [CrossRef]
18. Bacaicoa, J.; Ballesteros, T.; Arana, I.; Aginaga, J.; Latorre-Biel, J.I. Design, Manufacturing, Validation of a Multi-Orientation Tilt Test Bench for Testing Vehicles Rollover and Tests of ATV-Quad for Agricultural Applications. *Appl. Sci.* **2021**, *11*, 2575. [CrossRef]
19. Kim, W.S.; Siddique, M.A.A.; Kim, Y.J.; Jung, Y.J.; Baek, S.M.; Baek, S.Y.; Kim, Y.S.; Lim, R.G. Simulation of the Rollover Angle of a Self-Propelled Radish Harvester for Different Load Conditions. *Appl. Sci.* **2022**, *12*, 10733. [CrossRef]
20. Guo, J.; Yang, Y.; Memon, M.S.; Tan, C.; Wang, L.; Tang, P. Design and Simulation for Seeding Performance of High-Speed Inclined Corn Metering Device Based on Discrete Element Method (DEM). Scientific Reports. *Sci. Rep.* **2022**, *12*, 19415.
21. Shi, G.H.; Chen, Y.; Yang, Y.Z. BIW architecture multidisciplinary light weight optimization design. *J. Mech. Eng.* **2012**, *48*, 110–114. [CrossRef]
22. Chen, J.; Li, Z.; Fan, C.; Liu, W. Amplitude-requency Characteristic Analysis of Vehicle Vibration Response Based on MatLab. *J. Zhongyuan Univ. Technol.* **2011**, *22*, 45–49.
23. Yang, Y.B.; Ge, P.; Li, Q.; Liang, X.; Wu, Y. 2.5D Vibration of Railway-Side Buildings Mitigated by Open or Infilled Trenches Considering Rail Irregularity. *Soil Dyn. Earthq. Eng.* **2018**, *106*, 204–214. [CrossRef]
24. Jin, Q.; Luo, Q. MATLAB-Based Vibration Modeling of Two and Four Degrees of Freedom Vehicles. *Sci. Technol. Innov.* **2020**, 67–69.
25. Fang, X.; Tang, J. A Numerical Study of the Segregation Phenomenon in Granular Motion. *J. Vib. Control* **2007**, *13*, 711–729. [CrossRef]
26. Jung, J.; Kim, C. Scaling Law and Mechanism for the Formation of Stripe Patterns in a Binary Mixture of Granular Materials under Horizontal Vibration. *J. Korean Phys. Soc.* **2013**, *63*, 1937–1943. [CrossRef]
27. Cui, T.; Jing, M.; Zhang, D.; Yang, L.; He, X.; Wang, Z. Construction of the diserete element model for maize ears and verification of threshing simulation. *Trans. Chin. Soc. Agric. Eng.* **2023**, *39*, 33–46.
28. Khawaja, A.N.; Khan, Z.M. DEM Study on Threshing Performance of "Compression–Oscillation" Thresher. *Comp. Part. Mech.* **2022**, *9*, 1233–1248. [CrossRef]
29. Wang, W.; Liu, W.; Yuan, L.; Qu, Z.; He, X.; Lv, Y. Simulation and Experiment of Single Longitudinal Axial Material Movement and Establishment of Wheat Plants Model. *Trans. Chin. Soc. Agric. Mach.* **2020**, *51*, 170–180.
30. Wang, W.; Liu, W.; Yuan, L.; Qv, Z.; Zhang, H.; Zhou, Z. Calibration of discrete element parameters of wheat plants at harvest period based on EDEM. *J. Henan Agric. Univ.* **2021**, *55*, 64–72.
31. Da, Q.; Li, D.; Zhang, X.; Guo, W.; He, D.; Huang, Y.; He, G. Research on Performance Evaluation Method of Rice Thresher Based on Neural Network. *Actuators* **2022**, *11*, 257. [CrossRef]
32. Wang, Q.; Mao, H.; Li, Q. Modelling and Simulation of the Grain Threshing Process Based on the Discrete Element Method. *Comput. Electron. Agric.* **2020**, *178*, 105790. [CrossRef]
33. Zhang, D.; Yin, S.; Liao, H.; Jie, G.; Zhang, F.; Feng, T. Optimization of Millet Axial Flow Threshing and Separation Device Based on Discrete Element Method. *Teh. Vjesn.* **2021**, *28*, 1877–1884.
34. Zhang, D.; Yi, S.; Zhang, J.; Bao, Y. Establishment of Millet Threshing and Separating Model and Optimization of Harvester Parameters. *Alex. Eng. J.* **2022**, *61*, 11251–11265. [CrossRef]
35. Zhang, J.; Li, F. The monte carlo simulation on release homogeneity of suction-type metering device. *Trans. Chin. Soc. Agric. Eng.* **1994**, *10*, 56–62.
36. Cao, X.; Yang, D.; Du, X.; Jin, X.; Wang, J.; Huang, W. Design and experiment of pneumatic seeder unit based on EDEM. *J. Chin. Agric. Mech.* **2023**, *44*, 8–14.
37. Zhang, X.; Li, C.; Tang, Q.; Yang, Y.; Ma, Y. Vibration Properties of Spade Punch Planter of Maize. *J. Shenyang Agric. Univ.* **2009**, *40*, 732–735.
38. Wang, Y.; Li, C.; Wang, H. Experimental Sudy on Inflence of Vibration of Precision Spade Punch Planter of Maize on Sowing Quality. *J. Agric. Mech. Res.* **2008**, 124–126.
39. Gierz, Ł.; Markowski, P.; Choszcz, D.J.; Wojcieszak, D. Effect of Using Deflector in the Distributor Head of a Pneumatic Seed Drill on the Oat Seed Sowing Unevenness. *Sci. Rep.* **2023**, *13*, 15471. [CrossRef] [PubMed]
40. Han, D.D.; He, B.; Wang, Q.; Zhang, R.C.; Tang, C.; Li, W.; Zhang, L.H.; Lv, X.R. Optimization and Experiment of Seed-Filling Performance of the Air-Suction Densely Planted Seed-Metering Device Based on DEM. *Comp. Part. Mech.* **2024**. [CrossRef]
41. Han, D.; Zhang, D.; Jing, H.; Yang, L.; Cui, T.; Ding, Y.; Wang, Z.; Wang, Y.; Zhang, T. DEM-CFD Coupling Simulation and Optimization of an inside-Filling Air-Blowing Maize Precision Seed-Metering Device. *Comput. Electron. Agric.* **2018**, *150*, 426–438. [CrossRef]
42. Lu, W.; Huang, S.; Feng, T.; Cheng, J.; Hao, W.; Wang, H. Design and test of hole-type seed meter. *Hubei Agric. Sci.* **2020**, *59*, 149–152, 157.
43. Wang, W.; Song, L.; Shi, W.; Wei, D.; Chen, Y.; Chen, L. Design and Experiment of Air-suction Double-row Staggered Precision Seed Metering Device for Maize Dense Planting. *Trans. Chin. Soc. Agric. Mach.* **2024**, *55*, 1–13.